Eupalmerin acetate, a novel anticancer agent from Caribbean gorgonian octocorals, induces apoptosis in malignant glioma cells via the c-Jun NH_2-terminal kinase pathway

Arifumi Iwamaru,[1] Eiji Iwado,[1] Seiji Kondo,[1] Robert A. Newman,[2] Burnilda Vera,[3] Abimael D. Rodríguez,[3] and Yasuko Kondo[1]

Departments of [1]Neurosurgery and [2]Experimental Therapeutics, The University of Texas M. D. Anderson Cancer Center, Houston, Texas and [3]Department of Chemistry, The University of Puerto Rico, San Juan, Puerto Rico

Abstract

The marine ecosystem is a vast but largely untapped resource for potential naturally based medicines. We tested 15 compounds derived from organisms found in the Caribbean Sea (14 gorgonian octocoral–derived compounds and one sponge-derived compound) for their anticancer effects on human malignant glioma U87-MG and U373-MG cells. Eupalmerin acetate (EPA) was chosen as the lead compound based on its longer-term stability and greater cytotoxicity than those of the other compounds we tested in these cell types. EPA induced G_2-M cell cycle arrest and apoptosis via the mitochondrial pathway; it translocated Bax from the cytoplasm to the mitochondria and dissipated the mitochondrial transmembrane potential in both cell types. EPA was found to increase phosphorylated c-Jun NH_2-terminal kinase (JNK) by >50% in both U87-MG and U373-MG cells. A specific JNK inhibitor, SP600125, inhibited EPA-induced apoptosis, confirming the involvement of the JNK pathway in EPA-induced apoptotic cell death. Furthermore, 7 days of daily intratumoral injections of EPA significantly suppressed the growth of s.c. malignant glioma xenografts ($P < 0.01$, on day 19). These results indicate that EPA is therapeutically effective against malignant glioma cells *in vitro* and *in vivo* and that it, or a similar marine-based compound, may hold promise as a clinical anticancer agent. [Mol Cancer Ther 2007;6(1):184–92]

Introduction

More than 60% of anticancer drugs have originated from natural materials, such as plants, microbes, and marine organisms (1). Compared with totally synthetic drugs, compounds derived from natural sources tend to have well-defined three-dimensional structures, fitting biological target structures that are conserved across species; thus, natural compounds may act more specifically and have fewer or less severe adverse side effects than synthetics (2). Marine organism–derived medicines have several features that make them particularly suitable for consideration as sources of antineoplastic agents. For example, the vast majority of marine invertebrates have only primitive immune systems, and thus, they produce toxic substances as a form of defense; these substances would be expected to have high potency and low solubility, given that they are immediately and tremendously diluted by water (3). Therefore, an increasing number of compounds derived from sponges, algae, mollusks, and other marine organisms are being tested for their therapeutic effects against cancer and other diseases in clinical and preclinical trials (2–4).

Apoptosis is a cell death mechanism by which many chemotherapeutic drugs kill cancer cells (5). This process is characterized by chromatin condensation and fragmentation, cell shrinkage, and membrane blebbing. The Bcl-2 family, which consists of antiapoptotic and proapoptotic proteins, is the central regulator of apoptosis (6). When apoptosis is triggered, proapoptotic proteins, such as Bax and Bak, translocate from the cytoplasm to the mitochondrial membrane, where they interact with antiapoptotic proteins, such as Bcl-2 and Bcl-X_L, causing a loss of mitochondrial transmembrane potential and the release of cytochrome *c*. The release of cytochrome *c*, in turn, activates caspases, which then cause the apoptosis to occur.

Serine/threonine protein kinases, including the mitogen-activated protein kinases (MAPK) and Akt, are upstream molecules that play an important role in regulating the apoptotic response of a cell to various extracellular stimuli (7). Three MAPK groups have been identified: c-Jun NH_2-terminal kinase (JNK), extracellular signal-regulated kinase, and p38 (8). In most instances, JNK and p38 induce apoptosis, whereas extracellular signal-regulated kinase and Akt inhibit it.

Received 7/18/06; revised 10/31/06; accepted 11/27/06.

Grant support: USPHS U54 grant CA96033 (R.A. Newman, Y. Kondo, and A.D. Rodríguez) and Anthony D. Bullock III Foundation (S. Kondo and Y. Kondo). B. Vera is a scholar of the NIH-Minority Biomedical Research Support Program Support of Continuous Research Excellence Program/ Research Initiative for Scientific Enhancement Program of the University of Puerto Rico.

The costs of publication of this article were defrayed in part by the payment of page charges. This article must therefore be hereby marked *advertisement* in accordance with 18 U.S.C. Section 1734 solely to indicate this fact.

Note: A. Iwamaru and E. Iwado contributed equally to this work.

Requests for reprints: Yasuko Kondo, Department of Neurosurgery, Unit BSRB1004, The University of Texas M. D. Anderson Cancer Center, 1515 Holcombe Boulevard, Houston, TX 77030. Phone: 713-834-6214; Fax: 713-834-6257. E-mail: yaskondo@mdanderson.org

doi:10.1158/1535-7163.MCT-06-0422

Malignant glioma is the most common primary malignancy in the brain. Despite of aggressive combination of surgery, radiotherapy, and chemotherapy, the average survival time is <1 year from the diagnosis (9). This dismal outcome prompted the development of new drugs for the treatment of patients with malignant glioma. In the present study, we screened 15 compounds derived from organisms collected from the Caribbean Sea (14 from Caribbean gorgonian octocorals and 1 from a marine sponge) for cytotoxicity in human malignant glioma U87-MG and U373-MG cells. The lead compound, eupalmerin acetate (EPA), was then analyzed for its mechanism of action and found to induce apoptosis in the malignant glioma cells through activation of the JNK pathway. Furthermore, treatment of s.c. xenografts derived from U87-MG cells with EPA injections significantly inhibited tumor growth compared with the control treatment ($P < 0.01$).

Materials and Methods

Cell Lines

The human malignant glioma cell lines U87-MG and U373-MG were purchased from the American Type Culture Collection (Manassas, VA). These cell lines have different p53 status: U87-MG has wild-type p53 and U373-MG has mutant p53 (10). Cells were cultured and maintained in DMEM supplemented with 10% fetal bovine serum (Invitrogen, Carlsbad, CA), 4 mmol/L glutamine, 100 units/mL penicillin, and 100 μg/mL streptomycin at 37°C in 5% CO_2.

Marine Compounds

Specimens of the Caribbean gorgonian octocoral *Eunicea succinea* were collected at 25 m depth by SCUBA from Mona Island, Puerto Rico. The gorgonian was stored at 0°C immediately after collection and then frozen at −10°C on arrival, freeze dried, and kept frozen until extraction. The dried *E. succinea* (2.5 kg) was blended with MeOH-$CHCl_3$ (1:1), and after filtration, the crude extract was evaporated under vacuum to yield a residue (323 g) that was partitioned between hexane and H_2O. The hexane extract was concentrated to yield 171 g of a dark green oily residue, which was subsequently dissolved in toluene and filtered. The resulting filtrate was concentrated (169 g), loaded onto a large size exclusion column (Bio-Beads SX-3), and eluted with toluene. The combined terpenoid-rich fraction (thin-layer chromatography and ^1H nuclear magnetic resonance guided) was concentrated to a dark yellow oil (119 g) and chromatographed over a large silica gel column (3 kg) using 30% EtOAc in hexane. From this column, 14 fractions were obtained, the less polar of which consisted of complex mixtures of unidentified sterols and fatty acid derivatives and the known cembranolide diterpene EPA (13 g). The identification of analytically pure EPA was accomplished through detailed comparisons with the physical and chemical data previously reported for this compound (11–13).

All marine compounds were dissolved in DMSO (Sigma Chemical Co., St. Louis, MO). Stock solutions were made at a concentration of 50 mmol/L in DMSO and stored at −20°C.

Cell Proliferation Assay

Cells (1×10^4 per well, 100 μL) were seeded in 96-well flat-bottomed plates and incubated overnight in 5% CO_2-95% air at 37°C. The cells were then exposed to various concentrations of the marine compounds (0–100 μmol/L) for 72 h, and relative rate of surviving cells was determined using the 3-(4,5-dimethylthiazol-2-yl)-2,5-diphenyltetrazolium bromide reduction assay as described previously (14). Briefly, an aliquot of a 3-(4,5-dimethylthiazol-2-yl)-2,5-diphenyltetrazolium bromide solution (3 mg/mL in PBS) was added to each well (25 μL per 200 mL of medium), and the plate was incubated at 37°C for 2 h. Cells were then spun in a centrifuge at $300 \times g$ for 5 min, and the medium was removed carefully. A 50-μL aliquot of DMSO was added, and the absorbance of each well at 570 nm was measured on a microplate reader (Molecular Devices Corp., Sunnyvale, CA). The IC_{50} was defined as the concentration that inhibited the viability of cells by 50% compared with that of control cells. In the assays using a specific JNK inhibitor, SP600125, cells were pretreated with 5 μmol/L SP600125 for 1 h and then treated with EPA for 3 days. SP600125 and 3-(4,5-dimethylthiazol-2-yl)-2,5-diphenyltetrazolium bromide were purchased from Calbiochem (La Jolla, CA) and Sigma Chemical, respectively.

Flow Cytometry

For cell cycle analysis, cells were treated with EPA at 0, 5, 10, and 20 μmol/L for 72 h; fixed with ice-cold 70% ethanol; and then stained with propidium iodide using the Cellular DNA Flow Cytometric Analysis Reagent Set (Boehringer Mannheim, Indianapolis, IN). The stained cells were analyzed for DNA content using a FACScan (Becton Dickinson, San Jose, CA) as described previously (15). The percentages of cells in the sub-G_1, G_1, S, and G_2-M populations were determined with the CellQuest software program (Becton Dickinson).

For analysis of mitochondrial membrane potential, we used rhodamine 123 (Invitrogen), a cationic voltage-sensitive probe, as described previously (16). Cells were treated with 20 μmol/L EPA for 72 h, trypsinized, washed with PBS, and stained with 1 μmol/L rhodamine 123 in PBS by 1 h of exposure in the dark at 37°C. Cells were then washed, resuspended in PBS, and analyzed with the FACScan using CellQuest software.

Apoptosis Detection Assay

Tumor cells were seeded on Lab-Tek chamber slides (Nunc, Rochester, NY), incubated overnight, and then treated with 0 to 10 μmol/L EPA for 72 h and stained with the terminal deoxynucleotidyl transferase–mediated dUTP nick end labeling (TUNEL) technique using an ApopTag apoptosis detection kit (Invitrogen) as described previously (17). Two hundred cells were counted and scored for the incidence of positive staining under a microscope.

Immunocytochemical and Immunohistochemical Staining

To detect Bax translocation to the mitochondria, treated cells were fixed with 4% paraformaldehyde for 15 min and then incubated with 50 nmol/L MitoTracker Green FM probe (Invitrogen) for 20 min at room temperature while

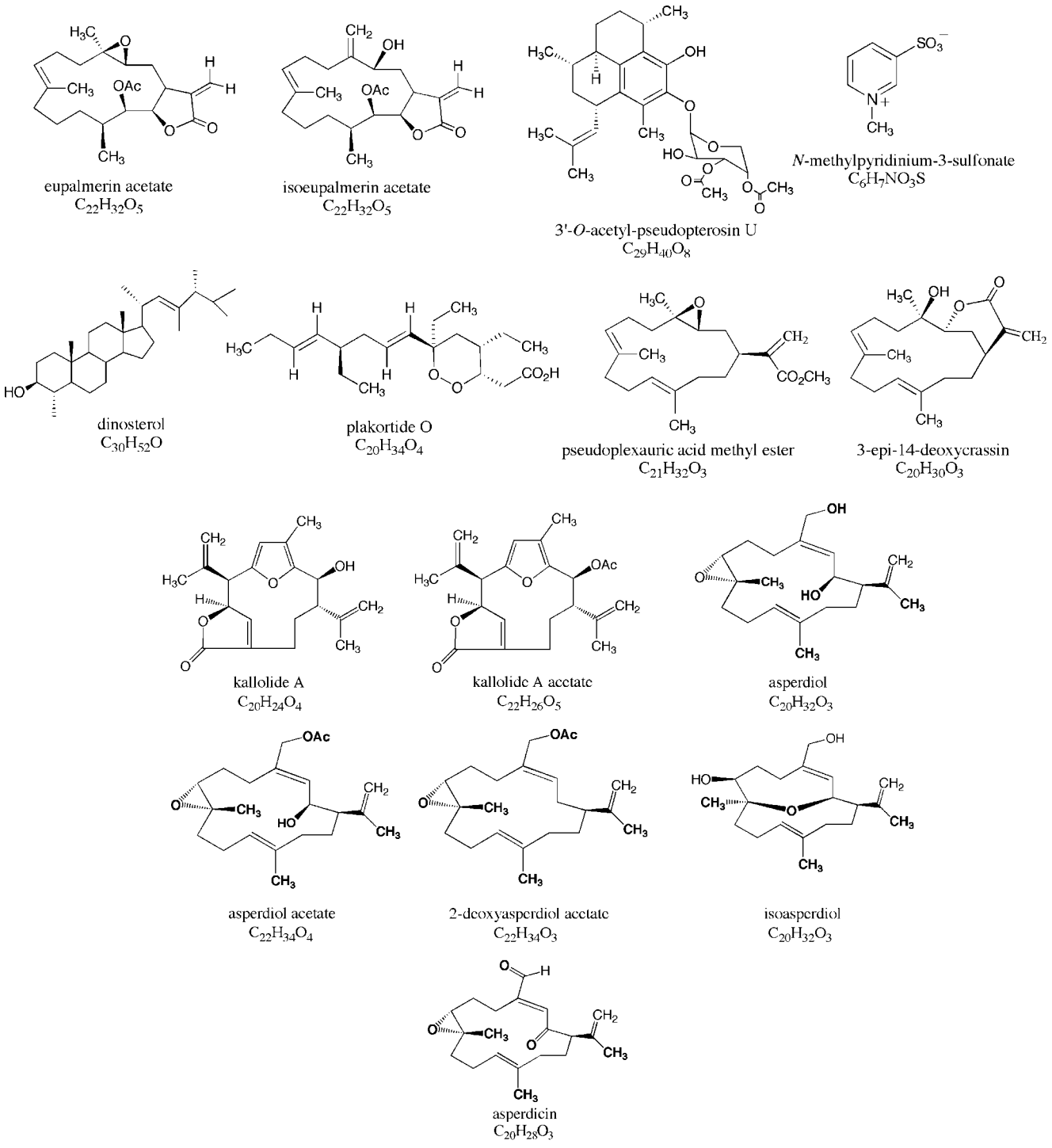

Figure 1. Structures of 15 potential anticancer compounds derived from organisms found in the Caribbean Sea. Plakortide O was derived from a marine sponge, *P. halichondroides*, whereas the remainders were derived from gorgonian soft corals (subclass Octocorallia).

being shielded from the light. PBS was used to remove excess probe. The samples were then blocked with 3% normal goat serum and incubated with anti-Bax (N-20) antibody (Santa Cruz Biotechnology, Santa Cruz, CA) at a 1:500 dilution in PBS containing 0.5% Triton X-100 (Sigma Chemical) overnight at 4°C. After a subsequent washing with PBS, the samples were visualized using Alexa Fluor 594–conjugated goat anti-rabbit IgG (Invitrogen).

For immunocytochemical and immunohistochemical staining, samples were fixed with 4% paraformaldehyde

Table 1. IC_{50} values of the top eight marine compounds studied

Compound	IC_{50} (μmol/L)	
	U87-MG	U373-MG
Plakortide O	4.0	4.0
EPA	5.1	6.9
Isoeupalmerin acetate	6.7	16.0
3′-O-acetyl-pseudopterosin U	14.0	37.0
3-Epi-14-deoxycrassin	25.8	64.2
Asperdicin	26.3	56.0
Pseudoplexauric acid methyl ester	74.7	>100
2-Deoxyasperdiol acetate	>100	57.5

for 15 min, washed with PBS, blocked with 3% normal goat serum, and incubated with anti–phosphorylated stress-activated protein kinase/JNK antibody (for phosphorylation at Thr^{183}/Tyr^{185}; Cell Signaling, Danvers, MA) or anti-Ki-67 antibody (Abcam, Cambridge, MA) in PBS overnight at 4°C. A secondary biotinylated antibody was then applied followed by incubation with avidin-biotin complex method solution (Vector Laboratories, Burlingame, CA). Samples were visualized by means of a standard diaminobenzidine reaction. The number of phosphorylated JNK-positive and Ki-67-positive cells per 100 cells was determined in each of three or more areas, which were chosen at random for each sample.

Immunoblotting

Cells were lysed in extraction buffer as described previously (18). Thereafter, for each immunoblot preparation, 40 μg protein was separated by SDS-PAGE (Bio-Rad, Richmond, CA) and transferred to a Hybond-P membrane (Amersham Co., Piscataway, NJ). The membranes were treated with antibodies against poly(ADP-ribose) polymerase (Cell Signaling), Bax, and Bcl-2 (Santa Cruz Biotechnology) and then subjected to immunoblotting. To detect upstream signaling for apoptosis, we also did immunoblotting using PathScan Multiplex Western Cocktail kits I, II, and III (Cell Signaling). Anti-Pin1 and anti-eIF4E antibodies were used as loading controls.

Animal Studies

All animal studies were done in the veterinary facilities of The University of Texas M. D. Anderson Cancer Center in accordance with institutional, state, and federal regulations and institutional and international ethical guidelines for the care and use of experimental animals. U87-MG cells (1.0×10^6 in 20 μL of serum-free DMEM) were inoculated s.c. into the right flank of 5- to 10-week-old female nude mice (six mice for each treatment group). Tumor growth was measured daily with calipers. Tumor volume was calculated as $(L \times W^2) / 2$, where L is the length in millimeters and W is the width in millimeters, as described previously (19). When the tumors reached a mean volume of 50 mm^3, intratumoral injections of EPA (50 mg/kg in 40 μL of DMSO and PBS) or injections of 40 μL of DMSO and PBS alone (vehicle) were given daily for 7 days. Tumor volume was measured every other day with calipers. Mice were euthanized by exposure to CO_2 when the tumor volume reached ≥1,500 mm^3 (for mice in the control group) or on day 19 (for mice in the EPA group). Tumors were removed, snap frozen, and kept at −80°C until use. Tumor specimens were sliced to a thickness of 10 to 20 μm with a cryostat, mounted on glass slides, fixed with 4% paraformaldehyde in PBS, and processed for immunohistochemical and TUNEL staining.

Statistical Analysis

The data were calculated as mean ± SD. Statistical analysis was done using the Student's t test (two tailed). Statistical significance was defined as $P < 0.05$.

Results

EPA Was Chosen for Its Potent Anticancer Effect and Stability

The 15 marine compounds isolated from organisms found in the Caribbean Sea and purified in our laboratory are shown in Fig. 1. These compounds were preselected based on their anticancer activity or on the anticancer activity of their derivative that had been assessed previously (20–22).

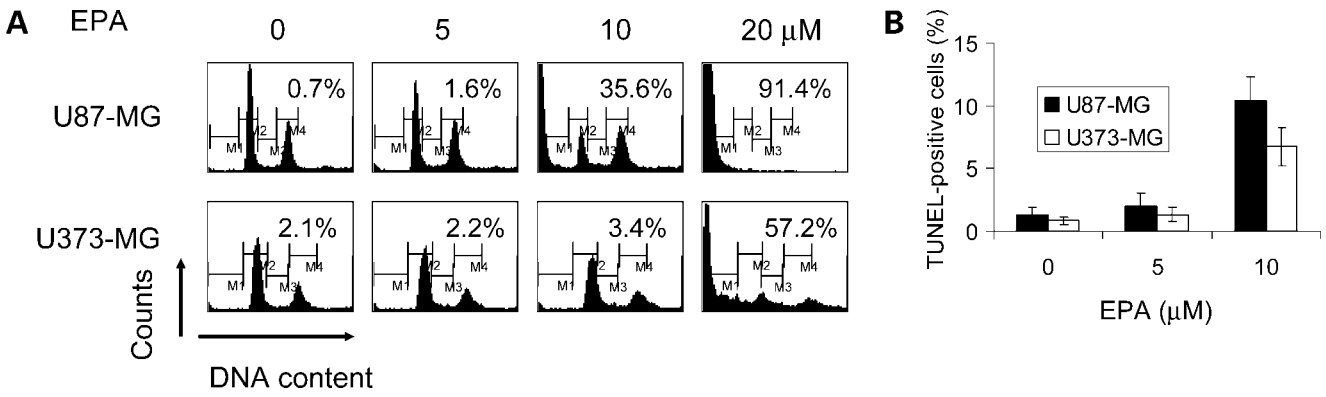

Figure 2. EPA induces G_2-M arrest and apoptosis in U87-MG and U373-MG cells. **A,** cell cycle analysis. Cells were treated with different concentrations of EPA for 72 h, incubated with propidium iodide, and subjected to flow cytometric cell cycle analysis. Percentage of the sub-G_1 population at each EPA concentration. Data are representative of three independent experiments. **B,** quantification of TUNEL-positive cells. Cells were treated as described above and subjected to the TUNEL assay. *Columns,* mean of triplicate experiments; *bars,* SD.

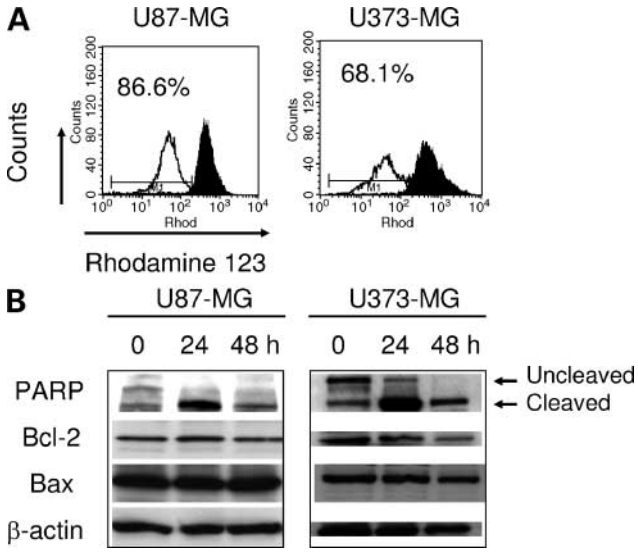

Figure 3. EPA dissipates mitochondrial transmembrane potential and induces apoptosis in U87-MG and U373-MG cells. **A,** cells were treated with 20 μmol/L EPA for 72 h, incubated with rhodamine 123, and subjected to flow cytometry. *Filled areas,* control cells treated with vehicle alone; *open areas,* cells treated with EPA. Percentage of cells with low rhodamine 123 staining in cells treated with EPA. **B,** Western blot analysis of apoptosis-associated proteins. Cells were treated with 10 and 20 μmol/L EPA, respectively; proteins were isolated at the indicated time points and subjected to Western blotting. *Arrows,* uncleaved and cleaved bands of poly(ADP-ribose) polymerase (*PARP*). β-Actin was used as the loading control. Data are representative of three independent experiments.

All the compounds but one were derived from gorgonian octocorals; plakortide O was derived from a marine sponge, *Plakortis halichondroides* (21, 22). All these compounds were coded and examined blindly for their relative cytotoxicity against human malignant glioma U87-MG and U373-MG cells. Cells were treated with each compound at 0 to 100 μmol/L for 72 h, and viability was determined using the 3-(4,5-dimethylthiazol-2-yl)-2,5-diphenyltetrazolium bromide assay. Table 1 shows the IC_{50} values of the eight most potent compounds in descending order of potency. The other seven compounds had IC_{50} values of >100 μmol/L in both cell types and were therefore considered not to be potent enough to serve as anticancer drugs for these cell types. Although plakortide O was the most potent of the tested compounds, its cytotoxicity significantly decreased after it was stored in solution for several weeks (IC_{50} value decreased from 4.0 to 31.0 μmol/L in U87-MG cells and from 4.0 to 15.4 μmol/L in U373-MG cells). The second most potent compound, EPA, was stable at least over several months, and it had IC_{50} values of 5.1 μmol/L for U87-MG cells and 6.9 μmol/L for U373-MG cells. This range of IC_{50} is compatible with that of cisplatin, which is in the range of 5 to 10 μmol/L for these cell types (data not shown). These results prompted us to focus on EPA and determine the mechanisms by which it asserted its anticancer effect.

EPA Translocates Bax to the Mitochondria and Induces Apoptosis in U87-MG and U373-MG Cells

To examine the effect of EPA on cell cycle and apoptosis, we treated cells with different concentrations of EPA for 72 h and did cell cycle analysis using flow cytometry (Fig. 2A). The percentage of cells in the sub-G_1 population, which indicates the level of cell death, increased from 0.7% at baseline to 35.6% and 91.4% in U87-MG cells treated with 10 and 20 μmol/L EPA, respectively. Similarly, the sub-G_1 population increased from 2.1% to 57.2% in U373-MG cells treated with 20 μmol/L EPA. For both cell lines, the percentages of cells in the G_1 population decreased and that of cells in the G_2-M phase increased in a dose-dependent manner after treatment with up to 10 μmol/L EPA (Fig. 2A), indicating that EPA also induced G_2-M arrest. Because apoptosis is a cell death mechanism by which many chemotherapeutic drugs kill cancer cells (5), we did TUNEL staining to examine whether EPA induces apoptosis in these cells (Fig. 2B). At 72 h after treatment with 10 μmol/L EPA, the percentage of TUNEL-positive cells increased from 1.3 ± 0.6% to 10.4 ± 1.9% in U87-MG cells and from 0.8 ± 0.3% to 6.7 ± 1.5% in U373-MG cells ($P < 0.05$ in both cell types). These results indicate that EPA induces apoptosis and G_2-M arrest in both cell types.

Bcl-2 family proteins regulate apoptosis by controlling the integrity of the mitochondrial membrane (6). To determine whether EPA induces apoptosis by loss of the integrity of the mitochondrial membrane through Bcl-2

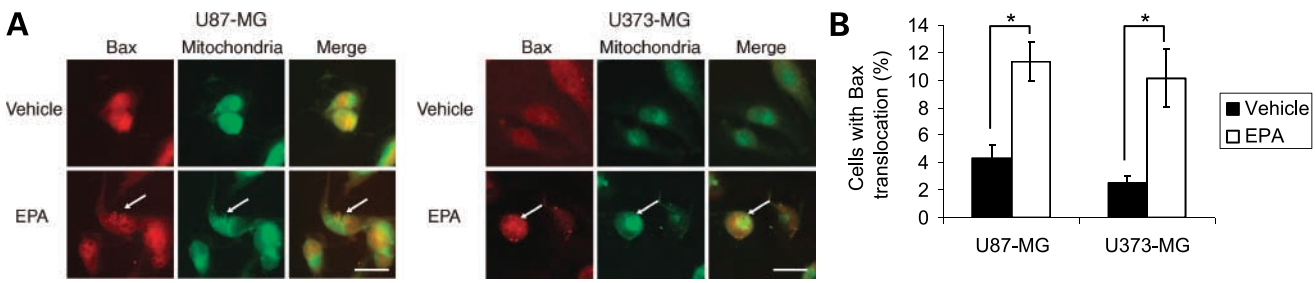

Figure 4. EPA translocates Bax to the mitochondria in U87-MG and U373-MG cells. Cells were treated with 10 μmol/L EPA for 24 h and then stained with an anti-Bax antibody and a mitochondrial marker. **A,** fluorescence micrographs of cells double stained with an anti-Bax antibody and a mitochondrial marker. *Arrows,* cells with colocalization of the two molecules. Bar, 10 μm. **B,** quantification of cells with Bax translocation to the mitochondria. Cells (100 per area, with three areas analyzed) that did and did not show Bax translocation to the mitochondria were counted, and the percentage of cells with Bax translocation were calculated. *Columns,* mean of triplicate experiments; *bars,* SD. *, $P < 0.01$.

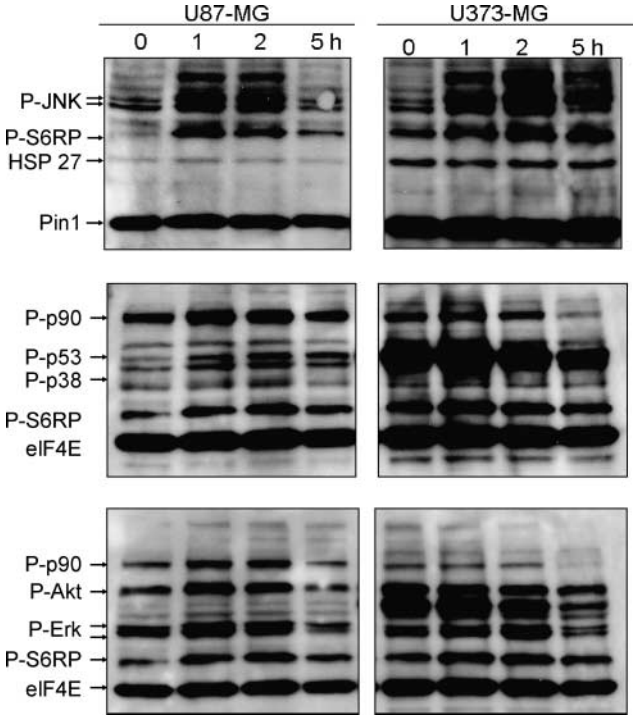

Figure 5. EPA transiently activates JNK in U87-MG and U373-MG cells. Representative Western blots prepared using PathScan Multiple Western Cocktail kits. U87-MG and U373-MG cells were treated with 10 and 20 μmol/L EPA, respectively, and proteins were then isolated at the indicated time points before being subjected to Western blotting. Pin1 and eIF4E were used as loading controls. Data are representative of two independent experiments.

family proteins, we measured the mitochondrial membrane potential using rhodamine 123 staining and did immunoblotting for poly(ADP-ribose) polymerase, Bcl-2, and Bax. EPA increased the proportion of cells with mitochondrial transmembrane potential dissipation to 86.9 ± 0.4% in U87-MG cells and to 70.1 ± 2.4% in U373-MG cells (Fig. 3A). Poly(ADP-ribose) polymerase was cleaved effectively at 24 h after EPA treatment in both cell types (Fig. 3B). The expression of Bcl-2 decreased after 48 h of EPA treatment in U373-MG cells, although it did not change in U87-MG cells (Fig. 3B). The expression level of Bax did not change during 48 h of EPA treatment in either cell type (Fig. 3B).

Although Bax remains inactivated, it localizes diffusely in the cytoplasm. Once apoptosis is induced, Bax translocates to the mitochondria, neutralizes antiapoptotic protein Bcl-2, changes its own conformation, and opens the mitochondrial pore, resulting in apoptosis (23). To determine whether Bax plays a role in EPA-induced apoptosis, we did double staining using an anti-Bax antibody and a mitochondrial marker (MitoTracker) in U87-MG and U373-MG cells. Twenty-four hours after EPA treatment, immunoreactivity to Bax showed punctate pattern and was colocalized with MitoTracker dye in both cell types (Fig. 4A). Quantification of double-stained cells showed that the percentage of the cells with Bax translocation to the mitochondria increased significantly from 4.3% to 11.3% in U87-MG cells and from 2.5% to 10.2% in U373-MG cells ($P < 0.01$ for both; Fig. 4B). These results indicate that EPA induces apoptosis in both cell types at least in part by activating the mitochondrial pathway and inducing Bax translocation to the mitochondria.

EPA Activates the JNK Pathway to Induce Apoptosis in U87-MG and U373-MG Cells

To determine which upstream signal pathways were activated or inhibited in EPA-induced apoptosis, we used PathScan Multiplex Western Cocktail kits. The following pathways were examined: the Ras/Raf/MAPK/extracellular signal-regulated kinase kinase/extracellular signal-regulated kinase/p90RSK pathway, the phosphatidylinositol 3-kinase/

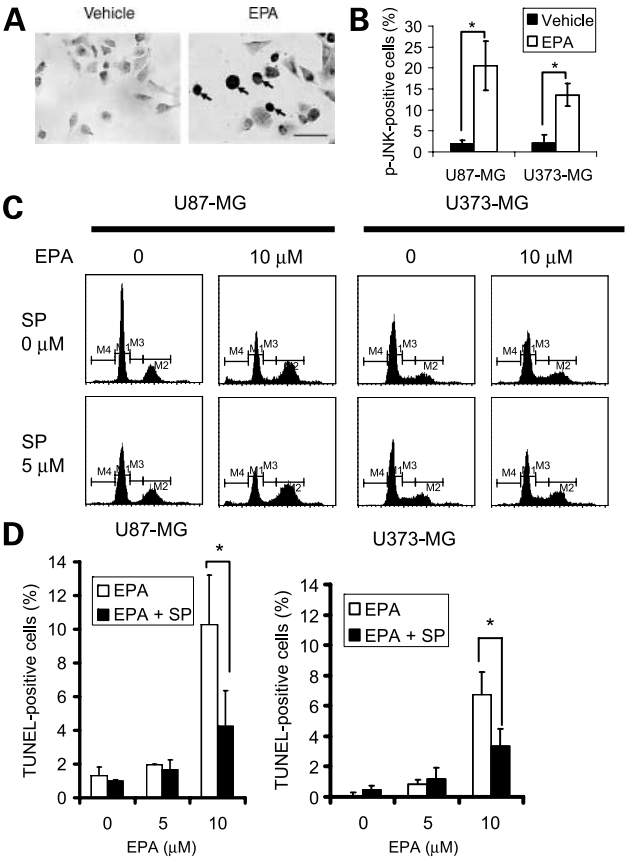

Figure 6. JNK is involved in EPA-induced apoptosis in U87-MG and U373-MG cells. **A,** cells were treated with 20 μmol/L EPA for 2 h and subjected to immunocytochemical staining using an anti–phosphorylated JNK antibody. *Arrows,* cells with positive phosphorylated JNK staining. Phosphorylated JNK-positive cells showed condensed nuclei and a rounded shape, indicating apoptosis. Bar, 50 μm. **B,** quantification of phosphorylated JNK (*p-JNK*)–positive cells in U87-MG and U373-MG cells treated with vehicle or 20 μmol/L EPA for 2 h. *Columns,* mean of triplicate experiments; *bars,* SD. *, $P < 0.01$. **C,** representative cell cycle analysis of U87-MG and U373-MG cells pretreated with 5 μmol/L SP600125 (*SP*) for 1 h and then treated with 10 μmol/L EPA for 72 h. **D,** quantification of TUNEL-positive cells. Cells were treated as described above and subjected to TUNEL staining. *Columns,* mean of triplicate experiments; *bars,* SD. *, $P < 0.05$.

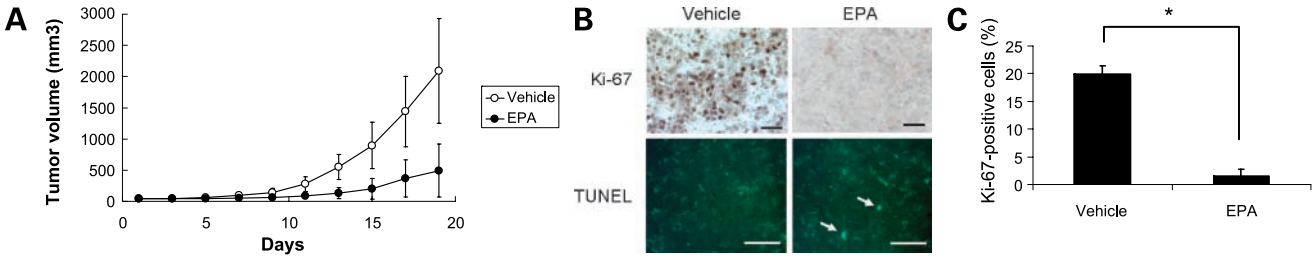

Figure 7. EPA significantly inhibits tumor growth *in vivo*. **A,** U87-MG cells (1×10^6) were injected s.c. into nude mice. When tumors reached 50 mm^3 in volume (day 1), intratumoral injections of EPA (40 mg/kg in DMSO and PBS) or vehicle were given every 24 h for a wk (seven doses). Tumor volume was measured every other day. *Points,* mean of six mice in each group; *bars,* SD. **B** and **C,** Ki-67-positive cells were detected significantly less often in the tumors treated with EPA than in tumors treated with vehicle. **B,** representative staining of tumor samples from mice treated with EPA or vehicle using an anti-Ki-67 antibody and the TUNEL assay. Excised tumors were snap frozen, sliced using a cryostat, and subjected to immunohistochemical staining using an anti-Ki-67 antibody or to fluorescein-tagged TUNEL assay. Bar, 50 μm. *Arrows,* apoptotic cells detected by TUNEL staining. **C,** quantification of Ki-67-positive cells in tumor specimens from mice treated with vehicle or EPA. Areas containing 100 cells were examined and the numbers of EPA-positive cells were determined; three or more areas were chosen at random for each sample. *Columns,* mean of triplicate sets of data; *bars,* SD. *, $P < 0.01$.

PDK1/Akt/mammalian target of rapamycin/p70S6K/S6RP pathway, the MAPK/extracellular signal-regulated kinase kinase kinase/MAPK kinase/JNK/c-Jun pathway, and the ASK1/MAPK kinase/p38MAPK/HSP27 pathway. The level of phosphorylated JNK increased by ~50% after 1 h of EPA treatment in U87-MG cells and by ~130% after 2 h of EPA treatment in U373-MG cells (Fig. 5). Levels of phosphorylated Akt and phosphorylated S6RP, the latter of which is a downstream target of Akt, increased in U87-MG cells by ~20% after 1 to 2 h of EPA treatment in U87-MG cells; in U373-MG cells, the level of phosphorylated Akt did not increase but that of phosphorylated S6RP did (by no more than 15%) after 1 to 2 h of EPA treatment (Fig. 5). The level of phosphorylated p90 decreased by ~35% after 5 h of EPA treatment in only U373-MG cells (Fig. 5). Collectively, these results indicate that EPA activates the JNK pathway in both U87-MG and U373-MG cells, suggesting that EPA induces apoptosis via the JNK pathway.

To confirm the involvement of the JNK pathway in EPA-induced apoptosis, we first used immunocytochemical staining to determine whether phosphorylated JNK was present in the cell nuclei. Two hours after treatment with EPA, some malignant glioma cells showed enhanced immunoreactivity to anti–phosphorylated JNK antibody in the nucleus; the cells also had begun to take on a rounded shape, which is characteristic of apoptosis (Fig. 6A). The percentage of phosphorylated JNK-positive cells increased significantly from 1.9% to 20.6% in U87-MG cells and from 2.2% to 13.6% in U373-MG cells after EPA treatment ($P < 0.01$ for both cell types; Fig. 6B). Further, the effect of a JNK-specific inhibitor, SP600125, on cell cycle and apoptosis was examined. Pretreatment of U87-MG and U373-MG cells with SP600125 did not inhibit EPA-induced G_2-M arrest (Fig. 6C). On the other hand, pretreatment with SP600125 significantly inhibited EPA-induced apoptosis from 10.3% to 4.3% in U87-MG cells and from 6.7% to 3.3% in U373-MG cells ($P < 0.05$ for both cell types; Fig. 6D). These results indicate that EPA induces apoptosis, at least in part, by activating the JNK pathway.

EPA Inhibits Tumor Growth in the S.c. Tumor Model

To determine whether the *in vitro* antitumor effect of EPA is recapitulated *in vivo*, we treated nude mice bearing s.c. tumors with EPA. When s.c. xenografts derived from U87-MG cells reached a mean volume of 50 mm^3 (defined as day 1), we injected EPA (50 mg/kg, dissolved in DMSO and PBS) or control vehicle (DMSO and PBS alone) directly into the tumors daily for 7 days and measured tumor size every other day until day 19. Mice treated with EPA had tumors ~80% smaller than those in mice treated with vehicle control on day 19 (mean volume: 2,090 ± 842 mm^3 in control mice and 492 ± 424 mm^3 in EPA-treated mice; $P < 0.01$; Fig. 7A). Tumors were removed on day 19 and assessed by TUNEL staining and immunohistochemical staining for phosphorylated JNK and the proliferation marker Ki-67. Some TUNEL-positive cells were detected in the tumors treated with EPA, but few were found in those treated with vehicle (Fig. 7B); phosphorylated JNK was not detected in tumors of either treatment group (data not shown). These results suggest that the majority of apoptotic cells were removed by phagocytes by day 19 and that EPA-induced JNK activation was transient, which was consistent with the results of immunoblotting analysis using PathScan (Fig. 5A). The expression of Ki-67 was strikingly inhibited in tumors treated with EPA relative to those treated with vehicle control (Fig. 7B); only 1.5% of treated cells stained positive for Ki-67, whereas 19.9% of control cells did so ($P < 0.01$; Fig. 7C). These results clearly indicate that EPA can inhibit the growth of malignant glioma cells *in vivo*.

Discussion

We have collected a large number of samples from organisms collected throughout the Caribbean Sea over the last 15 years and have isolated, purified, and tested >200 compounds for their anticancer and anti-inflammatory effects (21, 22, 24, 25). In the present study, EPA showed the best combination of cytotoxicity and stability among 15 such compounds we screened. *In vitro*, EPA induced

apoptosis effectively by activating a mitochondrial pathway (specifically the JNK pathway) in both U87-MG and U373-MG cells regardless of their p53 status. *In vivo*, the growth of s.c. xenograft tumors was remarkably inhibited by intratumoral injections of EPA, indicating that the agent also holds potential for clinical anticancer activity. Further work must, of course, involve development of a suitable formulation for either systemic administration or convection-enhanced delivery of the compound to animals and/or humans as well as appropriate toxicology tests. Convection-enhanced delivery is a recently developed technique of direct injection to increase drug uptake and distribution to large regions of the brain by applying a pressure gradient (26–28). With convection-enhanced delivery, chemotherapeutic and toxic materials can be delivered to brain tumors efficiently and homogeneously while limiting toxicity to surrounding areas and the whole body system. Our initial results as a pilot study, however, suggest that natural compounds derived from marine organisms, including EPA, are promising candidates for consideration as anticancer drugs.

JNK is a serine-threonine kinase and a member of the MAPK family. It modulates apoptotic pathways in response to a variety of extracellular stimuli (8). JNK induces apoptosis by means of several mechanisms, including the activation of transcription factors and through cytoplasmic substrates. For example, JNK activates the downstream transcription factor c-Jun, which increases transcription of Fas ligand, resulting in the induction of apoptosis (29). c-Jun is also implicated in the up-regulation of a proapoptotic member of the Bcl-2 family, Bim, which leads to apoptosis (30). JNK also directly phosphorylates Bim-related proteins, such as Bim and Bmf, which activate Bax and Bak, resulting in apoptosis (31). Further, JNK also phosphorylates 14-3-3 proteins and promotes Bax translocation to the mitochondria (32). Our results show that EPA mediates induction of apoptosis through activation of JNK mainly in the nucleus (Figs. 5 and 6A), suggesting the involvement of c-Jun activation.

Our immunoblot analysis revealed that the EPA-induced phosphorylation of JNK was transient in both U87-MG and U373-MG cells (Fig. 5). In U87-MG cells, the level of phosphorylated JNK after EPA treatment returned to the level in untreated cells by 5 h after the treatment. Indeed, no tumor cells expressed detectable phosphorylated JNK in EPA-treated s.c. tumors. Although some apoptotic cells were detected in the tumors treated with EPA, the incidence was very low. Instead, we found that the expression of Ki-67 was dramatically suppressed in treated tumors on day 19 (Fig. 7B). These results suggest the possibility that proliferating tumor cells had undergone apoptosis and had been removed during a relatively early period of EPA treatment and that only tumor cells that escaped apoptosis and had a low proliferation rate remained, indicating the potential for EPA to have a long-lasting antitumor effect *in vivo*.

In summary, we tested 15 compounds derived from Caribbean marine organisms, mainly from gorgonian soft corals, for their anticancer effects on U87-MG and U373-MG malignant glioma cells. Our lead compound, EPA, showed high potency in killing these cells: EPA induced apoptosis by translocating Bax to the mitochondria and depolarizing the mitochondrial membrane. Our analysis of upstream signaling revealed that EPA activates the JNK pathway in its induction of apoptosis; treatment with a JNK inhibitor was able to inhibit the cytotoxicity of EPA. Furthermore, EPA significantly inhibited the growth of s.c. xenograft tumors. Our results suggest that EPA may be a promising candidate for use as an anticancer drug.

Acknowledgments

We thank E. Faith Hollingsworth for her technical help.

References

1. Newman DJ, Cragg GM, Snader KM. Natural products as sources of new drugs over the period 1981-2002. J Nat Prod 2003;66:1022–37.

2. Paterson I, Anderson EA. Chemistry. The renaissance of natural products as drug candidates. Science 2005;310:451–3.

3. Amador ML, Jimeno J, Paz-Ares L, Cortes-Funes H, Hidalgo M. Progress in the development and acquisition of anticancer agents from marine sources. Ann Oncol 2003;14:1607–15.

4. Newman DJ, Cragg GM. Marine natural products and related compounds in clinical and advanced preclinical trials. J Nat Prod 2004; 67:1216–38.

5. Kaufmann SH, Earnshaw WC. Induction of apoptosis by cancer chemotherapy. Exp Cell Res 2000;256:42–9.

6. Cory S, Adams JM. The Bcl2 family: regulators of the cellular life-or-death switch. Nat Rev Cancer 2002;2:647–56.

7. Cross TG, Scheel-Toellner D, Henriquez NV, Deacon E, Salmon M, Lord JM. Serine/threonine protein kinases and apoptosis. Exp Cell Res 2000; 256:34–41.

8. Davis RJ. Signal transduction by the JNK group of MAP kinases. Cell 2000;103:239–52.

9. Reardon DA, Rich JN, Friedman HS, Bigner DD. Recent advances in the treatment of malignant astrocytoma. J Clin Oncol 2006;24:1253–65.

10. Badie B, Goh CS, Klaver J, Herweijer H, Boothman DA. Combined radiation and p53 gene therapy of malignant glioma cells. Cancer Gene Ther 1999;6:155–62.

11. van der Helm D, Ealick SE, Weinheimer AJ. 15(*R*)-acetoxy-6(*S*), 10(*S*)-dibromo-3a(*S*),4,7,8,11,12,13,14(*S*),15,15a(*R*)-decahydro-6,10,14-trimethyl-3-methylene-5(*R*),9(*R*)-epoxycyclotetradeca[b]2-furanone, $C_{22}H_{32}Br_2O_5$. Cryst Struct Commun 1974;3:167–71.

12. Ealick SE, Van der Helm D, Weinheimer AJ. The molecular structures and absolute configurations of eupalmerin acetate and eupalmerin acetate dibromide at low temperature. Acta Crystallogr 1975;B31:1618–26.

13. Fontán LA, Yoshida WY, Rodríguez AD. Application of 2D-NMR spectroscopy in the structural determination of marine natural products. Total structural assignment of the cembranoid diterpene eupalmerin acetate through the use of two-dimensional ^{1}H-^{1}H, ^{1}H-^{13}C, and ^{13}C-^{13}C chemical shift correlation spectroscopy. J Org Chem 1990;55:4956–60.

14. Yang P, Collin P, Madden T, et al. Inhibition of proliferation of PC3 cells by the branched-chain fatty acid, 12-methyltetradecanoic acid, is associated with inhibition of 5-lipoxygenase. Prostate 2003;55:281–91.

15. Kanzawa T, Iwado E, Aoki H, et al. Ionizing radiation induces apoptosis and inhibits neuronal differentiation in rat neural stem cells via the c-Jun NH_2-terminal kinase (JNK) pathway. Oncogene 2006;25: 3638–48.

16. Daido S, Kanzawa T, Yamamoto A, Takeuchi H, Kondo Y, Kondo S. Pivotal role of the cell death factor BNIP3 in ceramide-induced autophagic cell death in malignant glioma cells. Cancer Res 2004;64:4286–93.

17. Takeuchi H, Kondo Y, Fujiwara K, et al. Synergistic augmentation of rapamycin-induced autophagy in malignant glioma cells by phosphatidylinositol 3-kinase/protein kinase B inhibitors. Cancer Res 2005;65: 3336–46.

18. Daido S, Yamamoto A, Fujiwara K, Sawaya R, Kondo S, Kondo Y.

Inhibition of the DNA-dependent protein kinase catalytic subunit radiosensitizes malignant glioma cells by inducing autophagy. Cancer Res 2005;65:4368 – 75.

19. Ito H, Kanzawa T, Miyoshi T, et al. Therapeutic efficacy of PUMA for malignant glioma cells regardless of p53 status. Hum Gene Ther 2005;16: 685 – 98.

20. Rodriguez AD, Pina IC, Acosta AL, Ramirez C, Soto JJ. Synthesis of analogues of Eunicea γ-cembranolides containing cyclic ethers via saponification. J Org Chem 2001;66:648 – 58.

21. Rodríguez AD. The natural products chemistry of West Indian gorgonian octocorals. Tetrahedron 1995;51:4571 – 618.

22. del Sol Jimenez M, Garzon SP, Rodriguez AD. Plakortides M and N, bioactive polyketide endoperoxides from the Caribbean marine sponge *Plakortis halichondrioides*. J Nat Prod 2003;66:655 – 61.

23. Gross A, Jockel J, Wei MC, Korsmeyer SJ. Enforced dimerization of BAX results in its translocation, mitochondrial dysfunction, and apoptosis. EMBO J 1998;17:3878 – 85.

24. Cobar OM, Rodriguez AD, Padilla OL, Sanchez JA. The calyculaglycosides: dilophol-type diterpene glycosides exhibiting antiinflammatory activity from the Caribbean gorgonian *Eunicea sp.* J Org Chem 1997; 62:7183 – 8.

25. Shi YP, Rodriguez AD, Barnes CL, Sanchez JA, Raptis RG, Baran P. New terpenoid constituents from *Eunicea pinta*. J Nat Prod 2002;65: 1232 – 41.

26. Yang W, Barth RF, Adams DM, et al. Convection-enhanced delivery of boronated epidermal growth factor for molecular targeting of EGF receptor-positive gliomas. Cancer Res 2002;62:6552 – 8.

27. Degen JW, Walbridge S, Vortmeyer AO, Oldfield EH, Lonser RR. Safety and efficacy of convection-enhanced delivery of gemcitabine or carboplatin in a malignant glioma model in rats. J Neurosurg 2003;99: 893 – 8.

28. Lopez KA, Waziri AE, Canoll PD, Bruce JN. Convection-enhanced delivery in the treatment of malignant glioma. Neurol Res 2006;28: 542 – 8.

29. Kasibhatla S, Brunner T, Genestier L, Echeverri F, Mahboubi A, Green DR. DNA damaging agents induce expression of Fas ligand and subsequent apoptosis in T lymphocytes via the activation of NF-κB and AP-1. Mol Cell 1998;1:543 – 51.

30. Whitfield J, Neame SJ, Paquet L, Bernard O, Ham J. Dominant-negative c-Jun promotes neuronal survival by reducing BIM expression and inhibiting mitochondrial cytochrome *c* release. Neuron 2001;29: 629 – 43.

31. Lei K, Davis RJ. JNK phosphorylation of Bim-related members of the Bcl2 family induces Bax-dependent apoptosis. Proc Natl Acad Sci U S A 2003;100:2432 – 7.

32. Tsuruta F, Sunayama J, Mori Y, et al. JNK promotes Bax translocation to mitochondria through phosphorylation of 14-3-3 proteins. EMBO J 2004;23:1889 – 99.

Molecular Cancer Therapeutics

Eupalmerin acetate, a novel anticancer agent from Caribbean gorgonian octocorals, induces apoptosis in malignant glioma cells via the c-Jun NH_2-terminal kinase pathway

Arifumi Iwamaru, Eiji Iwado, Seiji Kondo, et al.

Mol Cancer Ther 2007;6:184-192.